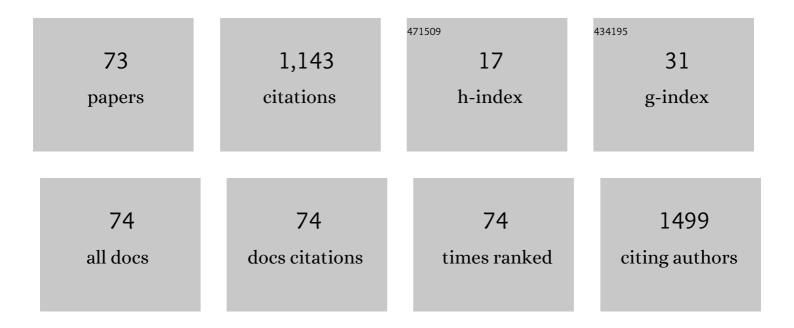
List of Publications by Year in descending order

Source: https://exaly.com/author-pdf/1807255/publications.pdf Version: 2024-02-01



#	Article	IF	CITATIONS
1	Synthesis of graphene crystals from solid waste plastic by chemical vapor deposition. Carbon, 2014, 72, 66-73.	10.3	136
2	Exciton radiative lifetime in ZnO nanorods fabricated by vapor phase transport method. Applied Physics Letters, 2007, 90, 013107.	3.3	74
3	Room-temperature growth of a carbon nanofiber on the tip of conical carbon protrusions. Applied Physics Letters, 2004, 84, 3831-3833.	3.3	65
4	Regenerated cellulose membrane as bio-template for in-situ growth of visible-light driven C-modified mesoporous titania. Carbohydrate Polymers, 2016, 146, 166-173.	10.2	63
5	Ferromagnetism in Cu-doped AlN films. Applied Physics Letters, 2009, 95, .	3.3	55
6	Transfer free graphene growth on SiO2 substrate at 250 °C. Scientific Reports, 2017, 7, 43756.	3.3	41
7	Direct Growth of Single Carbon Nanofiber onto Tip of Scanning Probe Microscopy Induced by Ion Irradiation. Japanese Journal of Applied Physics, 2006, 45, 2004-2008.	1.5	40
8	<i>In Situ</i> TEM Observation of Fe-Included Carbon Nanofiber: Evolution of Structural and Electrical Properties in Field Emission Process. ACS Nano, 2012, 6, 9567-9573.	14.6	31
9	Highly transparent and conducting C:ZnO thin film for field emission displays. RSC Advances, 2014, 4, 64763-64770.	3.6	31
10	Room-temperature growth of carbon nanofibers on plastic substrates. Surface Science, 2006, 600, 3663-3667.	1.9	29
11	Temperature dependent diode and photovoltaic characteristics of graphene-GaN heterojunction. Applied Physics Letters, 2017, 111, .	3.3	27
12	Photovoltaic Action in Graphene–Ga <sub>2</sub> O <sub>3</sub> Heterojunction with Deepâ€Ultraviolet Irradiation. Physica Status Solidi - Rapid Research Letters, 2018, 12, 1800198.	2.4	26
13	Preparation and catalytic evaluation of cytochrome c immobilized on mesoporous silica materials. Journal of the Ceramic Society of Japan, 2010, 118, 410-416.	1.1	25
14	Synthesis of uniform monolayer graphene on re-solidified copper from waste chicken fat by low pressure chemical vapor deposition. Materials Research Bulletin, 2016, 83, 573-580.	5.2	25
15	Photovoltaic Action With Broadband Photoresponsivity in Germanium-MoS <sub>2</sub> Ultrathin Heterojunction. IEEE Transactions on Electron Devices, 2018, 65, 4434-4440.	3.0	24
16	Effect of defects in ferromagnetic C doped ZnO thin films. Physica Status Solidi (B): Basic Research, 2012, 249, 1254-1257.	1.5	19
17	Ultraviolet light induced electrical hysteresis effect in graphene-GaN heterojunction. Applied Physics Letters, 2019, 114, .	3.3	18
18	Low temperature wafer-scale synthesis of hexagonal boron nitride by microwave assisted surface wave plasma chemical vapour deposition. AIP Advances, 2019, 9, .	1.3	18

#	Article	IF	CITATIONS
19	Influence of the Natural Zeolite Particle Size Toward the Ammonia Adsorption Activity in Ceramic Hollow Fiber Membrane. Membranes, 2020, 10, 63.	3.0	17
20	Direct observation of structural change in Au-incorporated carbon nanofibers during field emission process. Carbon, 2014, 75, 277-280.	10.3	16
21	Visualizing copper assisted graphene growth in nanoscale. Scientific Reports, 2014, 4, 7563.	3.3	16
22	Nitrogen doping effect on flow-induced voltage generation from graphene-water interface. Applied Physics Letters, 2018, 112, .	3.3	16
23	Role of Doped Nitrogen in Graphene for Flowâ€Induced Power Generation. Advanced Engineering Materials, 2018, 20, 1800387.	3.5	16
24	The role of solid, liquid and gaseous hydrocarbon precursors on chemical vapor deposition grown carbon nanomaterials' growth temperature. Synthetic Metals, 2021, 274, 116735.	3.9	16
25	Fabrication of transparent and flexible carbon-doped ZnO field emission display on plastic substrate. Physica Status Solidi - Rapid Research Letters, 2015, 9, 145-148.	2.4	15
26	Roomâ€ŧemperature ferromagnetism of Cuâ€doped ZnO films deposited by helicon magnetron sputtering. Physica Status Solidi (B): Basic Research, 2009, 246, 1243-1247.	1.5	14
27	Determination of Young's modulus of carbon nanofiber probes fabricated by the argon ion bombardment of carbon coated silicon cantilever. Carbon, 2011, 49, 4191-4196.	10.3	14
28	Observing Charge Transfer Interaction in Cul and MoS <sub>2</sub> Heterojunction for Photoresponsive Device Application. ACS Applied Electronic Materials, 2019, 1, 302-310.	4.3	13
29	Recent Developments in Carbon Nanotubes-Reinforced Ceramic Matrix Composites: A Review on Dispersion and Densification Techniques. Crystals, 2021, 11, 457.	2.2	13
30	Wafer-scale production of carbon nanofiber probes. Journal of Vacuum Science & Technology B, 2009, 27, 975.	1.3	12
31	The controlled fabrication of "Tip-On-Tip―TERS probes. RSC Advances, 2014, 4, 4718-4722.	3.6	12
32	Schottky Barrier Diode Characteristics of Graphene-GaN Heterojunction with Hexagonal Boron Nitride Interfacial Layer. Physica Status Solidi (A) Applications and Materials Science, 2018, 215, 1800089.	1.8	12
33	Low Temperature Direct of Graphene onto Metal Nanoâ€Spindt Tip with Applications in Electron Emission. Advanced Materials Interfaces, 2014, 1, 1300147.	3.7	11
34	Growth of uniform MoS2 layers on free-standing GaN semiconductor for vertical heterojunction device application. Journal of Materials Science: Materials in Electronics, 2020, 31, 2040-2048.	2.2	11
35	Roomâ€ŧemperature growth of ionâ€induced Si―and Geâ€incorporated carbon nanofibers. Physica Status Solidi (B): Basic Research, 2015, 252, 1345-1349.	1.5	10
36	Transparent and flexible field emission display device based on singleâ€walled carbon nanotubes. Physica Status Solidi - Rapid Research Letters, 2012, 6, 303-305.	2.4	9

#	Article	IF	CITATIONS
37	In situ transmission electron microscopy of Ag-incorporated carbon nanofibers: the effect of Ag nanoparticle size on graphene formation. RSC Advances, 2015, 5, 5647-5651.	3.6	9
38	Graphene formation at 150°C using indium as catalyst. RSC Advances, 2017, 7, 47353-47356.	3.6	9
39	Synthesis and Characterization of Li-C Nanocomposite for Easy and Safe Handling. Nanomaterials, 2020, 10, 1483.	4.1	9
40	Chemical state analysis using Auger parameters for XPS spectrum curve fitted with standard Auger spectra. Surface and Interface Analysis, 2018, 50, 1187-1190.	1.8	8
41	Switching isotropic and anisotropic graphene growth in a solid source CVD system. CrystEngComm, 2018, 20, 5356-5363.	2.6	8
42	Output density quantification of electricity generation by flowing deionized water on graphene. Applied Physics Letters, 2020, 117, .	3.3	8
43	Trifunctional Electrocatalytic Activities of Nitrogenâ€Doped Graphitic Carbon Nanofibers Synthesized by Chemical Vapor Deposition. ChemistrySelect, 2021, 6, 4867-4873.	1.5	8
44	Application of ion-induced carbon nanocomposite fibers to magnetic force microscope probes. Journal of Vacuum Science & Technology B, 2009, 27, 980.	1.3	7
45	Tuning the optical bandgap of multi-walled carbon nanotube-modified zinc silicate glass-ceramic composites. Ceramics International, 2021, 47, 20108-20116.	4.8	7
46	In situ fabrication of graphene from a copper–carbon nanoneedle and its electrical properties. RSC Advances, 2016, 6, 82459-82466.	3.6	5
47	Influence of MoS 2 ‧ilicon Interface States on Spectral Photoresponse Characteristics. Physica Status Solidi (A) Applications and Materials Science, 2019, 216, 1900349.	1.8	5
48	Formation of Effective Culâ€GaN Heterojunction with Excellent Ultraviolet Photoresponsive Photovoltage. Physica Status Solidi (A) Applications and Materials Science, 2019, 216, 1900200.	1.8	5
49	The Mo catalyzed graphitization of amorphous carbon: an <i>in situ</i> TEM study. RSC Advances, 2019, 9, 34377-34381.	3.6	5
50	High-Resolution Imaging of Plasmid DNA in Liquids in Dynamic Mode Atomic Force Microscopy Using a Carbon Nanofiber Tip. Japanese Journal of Applied Physics, 2011, 50, 08LB14.	1.5	5
51	Fabrication of Ion-Induced Carbon-Cobalt Nanocomposite Fibers: Effect of Cobalt Supply Rate. Journal of Nanoscience and Nanotechnology, 2011, 11, 10677-10681.	0.9	4
52	Synthesis of Freestanding WS <sub>2</sub> Trees and Fibers on Au by Chemical Vapor Deposition (CVD). Physica Status Solidi (A) Applications and Materials Science, 2018, 215, 1700566.	1.8	4
53	Effects of nitrogen-dopant bonding states on liquid-flow-induced electricity generation of graphene: A comparative study. Results in Physics, 2019, 12, 1291-1293.	4.1	4
54	Room-temperature graphitization in a solid-phase reaction. RSC Advances, 2020, 10, 914-922.	3.6	4

#	Article	IF	CITATIONS
55	Ferromagnetic and Optical Properties of Partially Cu-Doped ZnO Films. Zeitschrift Fur Naturforschung - Section A Journal of Physical Sciences, 2009, 64, 765-768.	1.5	3
56	Facile oneâ€step fabrication of highly transparent and flexible superhydrophobic substrate by roomâ€temperature ion irradiation method. Physica Status Solidi - Rapid Research Letters, 2012, 6, 430-432.	2.4	3
57	Controllable fabrication and characterization of conical nanocarbon structures on polymer substrate for transparent and flexible field emission displays. Physica Status Solidi - Rapid Research Letters, 2012, 6, 184-186.	2.4	3
58	Graphitization of Galliumâ€Incorporated Carbon Nanofibers and Cones: In Situ and Ex Situ Transmission Electron Microscopy Studies. Physica Status Solidi (B): Basic Research, 2020, 257, 2000309.	1.5	3
59	One-step synthesis of spontaneously graphitized nanocarbon using cobalt-nanoparticles. SN Applied Sciences, 2020, 2, 1.	2.9	3
60	Synthesis of MoS 2 Layers on GaN Using Ammonium Tetrathiomolybdate for Heterojunction Device Applications. Crystal Research and Technology, 2021, 56, 2000198.	1.3	3
61	Waste NR Latex Based-Precursors as Carbon Source for CNTs Eco-Fabrications. Polymers, 2021, 13, 3409.	4.5	3
62	Quantum limits to the electron field emission from tapered conductive sheets. Journal of Vacuum Science and Technology B:Nanotechnology and Microelectronics, 2010, 28, C2A64-C2A71.	1.2	2
63	Conducting polymer based hybrid structure as transparent and flexible field electron emitter. Physica Status Solidi - Rapid Research Letters, 2013, 7, 489-492.	2.4	2
64	Highly transparent and flexible field electron emitters based on hybrid carbon nanostructure. Physica Status Solidi - Rapid Research Letters, 2013, 7, 1080-1083.	2.4	2
65	Encapsulation of transition metal dichalcogenides crystals with room temperature plasma deposited carbonaceous films. RSC Advances, 2017, 7, 41136-41143.	3.6	2
66	Development of oxide nanofiber–tipped cantilever as a substrate for crossâ€sectional transmission electron microscopy analysis. Surface and Interface Analysis, 2018, 50, 1122-1126.	1.8	2
67	Angular Distribution of Sputtered Ions from HfN by Ar+ Ion Bombarment. Hyomen Kagaku, 2005, 26, 449-453.	0.0	2
68	Influence on Electrochemical Reactivity and Synthesis of Stainless Steel/Nitrogen-Doped Carbon Nanofibers. Journal of Physical Chemistry C, 2021, 125, 25197-25206.	3.1	2
69	Effect of surface morphology on the field emission property of ZnO films. Physica Status Solidi C: Current Topics in Solid State Physics, 2014, 11, 1349-1352.	0.8	1
70	Temperature dependence of catalytic activity in graphene synthesis for Sn nanoparticles. Journal of Materials Science: Materials in Electronics, 2019, 30, 12796-12803.	2.2	1
71	Sinterâ€Crystallization and Optical Characterization of Dy <sup>3+</sup> : ZnOâ€B <sub>2</sub> O <sub>3</sub> â€RHA Glassâ€Ceramics. Macromolecular Symposia, 2022, 401, 2100316.	0.7	1
72	Quantum limits to the electron field emission from tapered conductive sheets. , 2009, , .		0

#	Article	IF	CITATIONS
73	Fabrication of well ordered Zn nanorod arrays by ion irradiation method at room temperature and effect on crystal orientations. , 2010, , .		0